SAE INTERNATIONAL

2022-24-0007

Published: September 16, 2023

Optimization of Water Cooling for High Power Density Electrical Machines

Christoph Ellenrieder[1], Benedikt Reick[1], and Marcus Geimer[2]
[1]Ravensburg-Weingarten University
[2]Karlsruhe Institute of Technology

Citation: Ellenrieder, C., Reick, B., Kaufmann, A., and Geimer, M., "Optimization of Water Cooling for High Power Density Electrical Machines," SAE Technical Paper 2022-24-0007, 2022

DOI: https://doi.org/10.4271/2022-24-0007

Received: 17 May 2022 Revised: 11 Jul 2022 Accepted: 13 Jul 2023

Abstract

The power density of electric machines is a critical factor in various applications, i.e. like the power train. A major factor to improve the power density is boosting the electric current density, which increases the losses in the limited volume of the electric machine. This results in a need for an optimized thermal design and efficient cooling. The dissipation of heat can be achieved in a multitude of ways, ranging from air cooling to highly integrated cooling solutions. In this paper, this variety is shown and analyzed with a focus on water cooling. Further various structures in electric machines are presented.

A planar testbench is built to systematically analyze water cooling geometries. The focus lies in providing different power loss distributions along cooling channels, accurate temperature readings in a multitude of locations, as well as the pressure drop across the channel. The test bench results are aligned with simulations and simplified analytical evaluation to support the development process.

The main goal in this paper is to determine temperature gradients in the material close to the stator to quantize the potential for future cooling jacket designs. One question ,to answer is: How large the gradient is considering a realistic power loss distribution. Another sensible point are the different thermal expansions of aluminum used in cooling jackets and the steel core of the stator. This can be bypassed by using a steel cooling jacket. In this case, the performance of a steel cooling jacket compared to an aluminum version is investigated and also if light weight construction can compensate the lower thermal conductivity of steel.

After the analysis, an outlook about future changes of the measurement methods are given and first potentials for future cooling jackets are proposed.

Introduction

In vehicles, a key factor for successful electrification is to achieve a small electric machine size. In mobile machinery, electric machines are competing with high power density hydraulic systems [1, 2]. In the state of the art propulsion systems in general [3] and also in railway applications [4] a high power density is aimed for. For once the size determines the space needed for a drive but also influences dynamic properties through inertia.

Power Density of Electric Machines

Usually for a first construction space analysis Equation (1) can be used to calculate the length of the iron core l_{fe} and the air gap diameter d_{air} using the torque demand T and either the rotary thrust σ in $\frac{kN}{m^2}$ or the utilization number C in $\frac{kW \cdot min^{-1}}{m^3}$. Values for these vary widely depending on the resulting size and highly on the cooling system as can be seen in [5].

$$T = \frac{\pi}{2} \cdot \sigma \cdot d_{air}^2 \cdot l_{Fe} = \frac{1}{2\pi} \cdot C \cdot d_{air}^2 \cdot l_{Fe} \tag{1}$$

Equation (2) describes the rotary thrust underlining the importance of the cooling system. It depends on the maximum magnetic flux B, which is a material dependent constant and the current density A which is mainly thermally limited. The current density also depends linearly on the stator diameter. As can be seen, cooling is a main influencing factor for increasing the power density and thus one of the key factors to improve the build volume and performance of electric machines.

$$\sigma = \frac{z_c \cdot I_c}{\pi \cdot d_{air}} \cdot B = A \cdot B \tag{2}$$

Another way to increase the power density of an electric motor is to reduce the output torque and increase the maximum speed with the consequence of additionally needed transmission [5, 6].

Power Losses and Temperature Distribution in Electric Machines

Based on a first design, a more detailed analysis which, carries out calculations of the electromagnetic behavior, can be done. From these results, various sets of details can be extracted, i.e. the developed torque but also resulting losses at different operating points and their distribution within the electric motor.

The losses P_{losses} can be split in mechanical losses P_{mech} , losses in the stator P_{st}, and rotor losses P_{ro}, see Equation (3). The mechanical losses can be divided into air friction losses and bearing losses, which are mainly located at the end faces. P_{st} can be broken down in the losses, in the winding $P_{st,cu}$ and iron losses $P_{st,fe}$ induced in the stator core. Up to 20 % of the winding losses are in the winding heads, which are also located at the end faces [7]. The rotor losses are the sum of the rotor iron losses $P_{ro,fe}$ and either losses in the rotor winding $P_{ro,cu}$ or losses in the magnets $P_{ro,mag}$ depending on machine technology.

$$\begin{aligned} P_{losses} &= P_{mech} + P_{st} + P_{ro} \\ &= P_{mech} + P_{st,Cu} + P_{st,fe} + \cdots + P_{ro,fe} \\ &\quad + P_{ro,mag/cu} \end{aligned} \tag{3}$$

The distributed power losses in the stator along the electric motor create hotspots as presented in [8] and pictured in Figure 1 a). The temperature of the stator winding is significantly higher in the end winding due to high partial losses in this area. This is due to missing metal to metal contacts for good thermal conductivity and many conductors located in the end faces due to the interconnecting function of the end windings [3]. High power density applications either use water, some sort of oil or sometimes both fluids as coolant [9]. A simple design for water cooling is a circumferential system with a cooling jacket containing channels for the coolant. The temperature distribution depicted in Figure 1 hotspots in the area of the end winding. A common cooling jacket design is shown in Figure 1 b) where the fluid flows along a spiral path around the stator core. At the inlet, the water is relatively cool with temperature T_{low} and heats up continuously until it exits at the outlet with a higher temperature T_{high}.

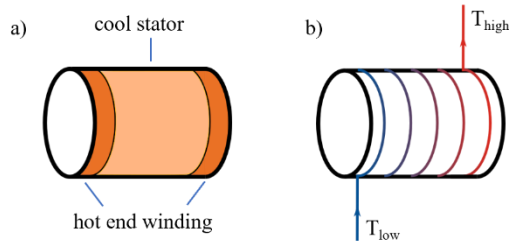

Figure 1: Flow concepts of cooling jackets
a) Loss distribution along the stator axis b) Conventional spiral

As the number of applications for electric machines rises cooling jacket designs, are developed and thoroughly looked into (i.e. [7]). In Figure 2 a) the meandering follows a circumferential path whereas in Figure 2 b) the axial direction is used. These concepts are often used due to better manufacturability. The possibility of splitting the coolant flow to each side of the stator jacket is sometimes also used to reduce temperature differences. In [10] the axial meander is examined. The resulting concept c) with two coolant inlets at the outer side of the jacket and one outlet in the middle works best from their investigated configurations. The design is able to reduce the temperature in the area of the end windings by up to 15 K, compared to the initial concept, and also reduces the axial temperature gradient. This means that the temperature at both end faces is on the same level. This is beneficial, because the insulation on the conductors limits the maximal current according to the insulation classes from IEC 34-1. If now both end faces reach that limit at the same time, the power density of the machine can be significantly increased.

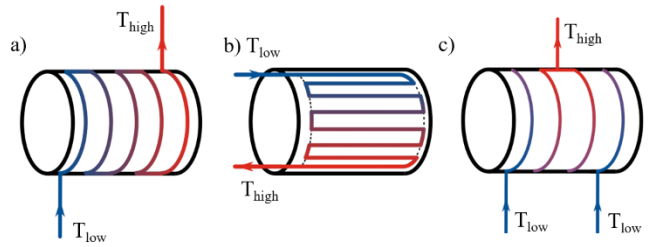

Figure 2 Flow concepts for cooling jackets
a) Circumferential meander b) Axial meander c) Distributed spiral

State of the Art Cooling Systems

A vast amount of different cooling systems are already used or are being developed. [9] and [11] give an overview and some evaluations. In the following paragraphs, the promising and common concepts are presented to give an outline on possible solutions.

Aims of the ongoing research are to optimize existing structures as i.e. the meander from Figure 2 b) where in the small radii of the rerouting high pressure losses occur. This is tackled in [12] where the geometry of the cooling channel is modified in a way that the flow velocity is always constant and the pressure drop is decreased.

In [13] wing profiles similar to NACA profiles are presented, see also Figure 3 a). A similar approach is used in the VW e-Up and e-Golf in a die casting motor housing which is shown in Figure 3 b) [14, 15].

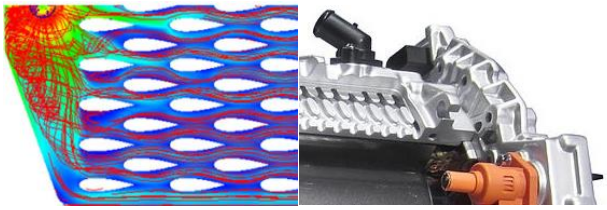

Figure 3 Structures in cooling jackets
a) NACA profiles[13] b) Oval profiles in a die casting motor housing[15]

An alternative is a highly integrated cooling concept, where oil is pumped through hollow conductors using high-pressure pumps [16]. Other concepts integrate the cooling system in the stator slots in between the conductors [17] or use heat pipes [18]. All those concepts apply major changes to the electric motor system, which require additional integration effort. High pressure losses can also cause larger parasitic power losses or may cause constipations in the cooling system.
Possibilities by modification of local structures to increase cooling performance using vortex generators are looked into in [19] in general and in [20] especially for electric motors.
Further research on cooling structures is also done in the field of power electronics. In these applications the power losses occur very concentrated in a chip. For that reason microchannels and pin fins [21] are a viable option.

Evaluation of Cooling Structures

As shown in the previous chapter, many different approaches have been investigated to improve the cooling performance of electric machines. Mayor boosts in overall performance, can be achieved by various concepts with most of them focusing on the cooling system in a global way.

One focus of this paper lies in keeping the changes to the electric machine itself low and to optimize the concept of the cooling jackets to improve cooling performance. Therefor a way to assess the problem of temperature gradients is investigated. Knowing the temperature gradient can be used to optimize future cooling structures and their distribution to minimize the gradient. This results in a better thermal utilization and thus a higher power density.

Another interesting issue is the pairing of aluminum cooling jackets and the sheet metal package of the stator. Both having different thermal expansion factors results in mechanical stress. For proper press fittings, in a wide temperature range, a huge overlap is necessary. This can be bypassed by using a steel cooling jacket. Furthermore in next steps it is planed to create special cooling structures using additive manufacturing using steel as source material. For this reason it is interesting how a steel cooling jacket performs compared to an aluminum version. Because steel has worse thermal conductivity than aluminum compensating but better mechanical properties light weight construction can be used to compensate this factor.

For these investigations, a test bench is designed, set up and measurements using different metal materials and different loss distributions are performed. The measurements are then interpreted and further on next steps are sketched out.

Test Bench for Systematic Evaluation of Cooling Structures

Problem Reduction and Requirements

To understand the problem of thermal gradient, adding cooling structures and optimizing the distribution of the structures systematic research has to be carried out. For this, a testbench is set up. The testbench is designed so that it closely resembles effects occurring in the cooling of electric machines. This results in multiple requirements:

1. An analytical description for the evaluation of the basic setup needs to be available
2. Imprinting a power loss profile along the cooling channel to simulate the power loss distribution along the channel is possible
3. Simple switching of the test objects needs to be possible
4. Measurements, close to the power loss surface, have to be possible

Regarding the first requirement, the design has to be kept simple, to be able to find analytical descriptions and to be able to systematically assess different structures. This would not be possible, when directly using cooling jackets as shown in Figure 1 and Figure 2. Multiple effects occur in these structures, like different coolant paths along loss profiles or a distributed inlet structure. For that reason, it was decided to create a planar test bench as it is presented in Figure 4. The device under test (DUT) is mounted in the middle on top of a segmented heating plate containing multiple heating cartridges which fulfill requirement number two. Exchanging DUTs can be done with relatively low effort, because of the modular design of the testbench. The DUT is mounted to the heat plate for good thermal contact and the symmetric in- and outlet containing sensors for coolant measurements can be easily detached.
To fulfil the last requirement, PT100 sensors with a diameter of 1 mm are mounted in the bottom wall of the DUTs at all point of interest. In general there are seven sensors in the middle of the channel directly above the heating cartridges. For further details, i.e. heat distribution across the channel width, additional sensor are added.

For the geometric parameters of the test bench an electric motor with water cooling and known parameters from project partner Fischer Elektromotoren GmbH was chosen. The total power of the heating cartridges is defined according to the power losses P_{losses} with a maximum peak of 2167 W occurring in the motor. The contact area $A_{contact}$ between the DUT and the heating plate is set to 257.6 cm² which correlates to the outer surface of the stator core. The point for peak performance and S1-operating point as well as the resulting power losses can be seen in Table 1.
For design reliability a power loss of 700 W is assumed in testing for the S1 operating point and 1400 W for an S6 artificial cycle.

Table 1 Motor data TI085-052-070-04B7S-07S04BE2
with kind courtesy of Fischer Elektromotoren GmbH

Operating point	Torque Nm	Speed min-1	Mechanical Power kW	Winding losses W	Power losses W
Nominal – S1	11.1	13250	15.4	254	617
Peak	29.1	11600	35.3	1843	2167

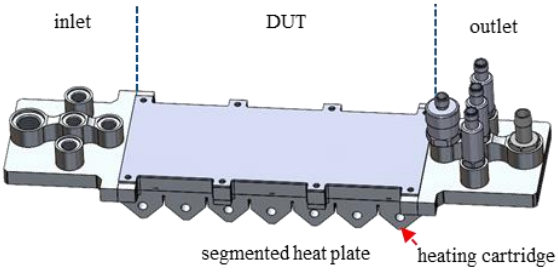

Figure 4 Test bench setup

Measurement Setup and Sensor Specification

The measurement system consists of a combination of self-developed hardware and a Raspberry Pi 4. The hardware is designed with dedicated channels measuring the resistance of the PT100 resistance temperature detectors (RTD) with a resolution of 0.03125 K and the ability to use 2, 3 and 4-wire measurement. In this setup, the 4-wire measurement is chosen with PT100 sensors of class A with a deviation of ±0,15 K according to IEC 751 [22]. The coolant temperature is measured with three sensors at the inlet and three sensors at the outlet with an accuracy of $\pm 0.3\ K$. Pressure drop is acquired with two absolute pressure sensors with an accuracy of 0.1 %. The mounting positions are marked in Figure 5.

When looking at the cross section of the test bench, one can see that the coolant is entering from the left where the inlet sensors are mounted. The coolant then enters the DUT which has a contact area to the heating plate in the bottom. The coolant exits to the right where the outlet sensors are mounted.

The measurement of the equivalent stator – cooling jacket interface is performed with the PT100 sensors. The sensor elements are positioned in holes created by wire discharge machining (EDM). This allows measurement in the wall, with 5 mm thickness, close to the contact area (orange line, Figure 5), inbetween the cooling channel and the segmented heating plate.

The channel in the reference DUT has a thin gap geometry which is $w = 90\ mm$ wide and $s = 4.5\ mm$ high, staying close to the cooling geometry of the reference motor. For investigations of the basic effects no structures are embedded in this channel.

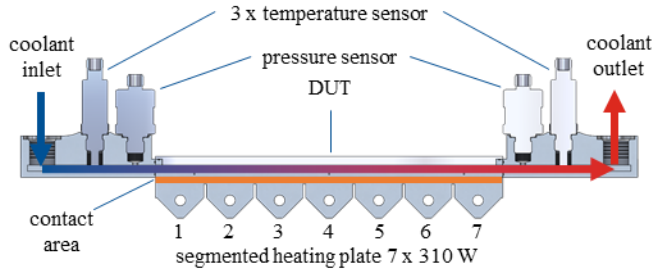

Figure 5 Cross section of the designed test bench

The heating plate is designed to contain seven heating cartridges which are embedded in separate segments. Those segments are divided by slots. A quite sharp power loss distribution can be imprinted in this way and the thermal capacity is as low as possible. Each segment allows up to 310 W of losses which can be controlled by a 24 Volt-PWM. The desired and resulting current and thus the power for a set of duty cycles is presented in Table 2. The accuracy of the set power is 3 % for 6.2 W power settings and 2 % at 310 W.

Table 2 Verification of 24 V heating cartridge power

Duty Cycle	2% 6.2 W	20% 62 W	50% 155 W	80% 248 W	100% 310 W
Current - $I_{desired}$ in A	0.258	2.583	6.458	10.333	12.917
Current - $I_{meassured}$ in A	0.250	2.540	6.330	10.180	12.700
Deviation	3 %	2 %	2 %	1 %	2 %

The temperature sensors are calibrated to 0 °C using ice water and a calibration duration of 100 s with a sampling rate of 1 s. After calibration, the sensors are mounted in the DUT. With no induced losses the standard deviation σ of all sensors is 0.0336 K.

Both pressure sensors, inlet and outlet, were calibrated to the same ambient pressure to increase the reliability in differential pressure calculation.

Verification Using Analytical Approaches

To be able to rely on measurements as reference geometry, the so called thin gap is chosen. For this geometry both, analytical descriptions for pressure drop and thermal behavior are available.

Analytic Calculation of Pressure Drop

There are various descriptions to calculate the pressure drop for a thin gap. The approach from [23] is used for this chapter.

The Reynolds number can be calculated using Equation (4), where ρ is the density of the coolant in kg/m^3, u is the mean coolant speed in m/s, D_H is the hydraulic diameter in m and $\nu_{coolant}$ is the kinematic viscosity in m^2/s.

$$Re = \frac{\rho \cdot u \cdot D_H}{\nu} \tag{4}$$

In the case of a parallel plate duct the hydraulic diameter D_H can be set to $D_H = 2 \cdot s$ where s is the height of the channel, here $s = 4.5\ mm$. With 5 l/min the resulting Reynolds number Re is in the range of 1830, which is by definition in the laminar region, but due to the inlet flow structure it might also be turbulent. The Darcy friction factor for turbulent flow f_t can be calculated iteratively and the laminar frictrion factor f_l using Equation (5). For turbulent flow additionally the surface roughness ϵ is needed.

$$\frac{1}{\sqrt{f_t}} = -2 \cdot \log_{10}\left[\frac{\epsilon}{3.7 \cdot D_H} + \frac{2.51}{Re \cdot \sqrt{f_t}}\right], \qquad f_l = \frac{64}{Re} \tag{5}$$

Resulting from this friction factor, the coefficient of resistance $\zeta_{channel}$ can be calculated using the Darcy factor according to Equation (6).

$$\zeta_{channel} = \frac{l}{D_H} \cdot f_t \tag{6}$$

Finally the pressure drop Δp can be calculated using Equation (7), using the coolant density $\rho_{coolant}$ and the average fluid velocity $u_{coolant}$.

$$\Delta p = \frac{1}{2} \cdot \rho_{coolant} \cdot \zeta_{channel} \cdot u_{coolant}^2 \tag{7}$$

Plausibility Check Using the Law of Conservation of Power

For checking the plausibility of measurements Equation (8), can be used. $\dot{m}$ is the mass flow rate in kg/s, c_p is the heat capacity of the coolant in $kJ/(kg \cdot K)$, and ΔT is the temperature difference between coolant inlet and outlet temperature in K.

Taking this into account and using the coolant inlet and outlet temperature sensors on the test bench each measurement can be evaluated for plausibility.
This can only be done in a stationary state due to the thermal capacities in the system. Important for this measurement is that no energy is dissipated through convection or radiation. For this reason the test bench is insulated using high temperature insulation material.

$$P = \dot{m} \cdot c_p \cdot \Delta T \tag{8}$$

Results

Using the previously described test bench a first set of measurements is performed. For this test series two DUTs with same channel geometry but different materials are studied. The first DUT is manufactured using aluminum 7075. The outer geometry being CNC milled and the channel geometry cut using wire EDM. The second DUT is made from stainless steel using additive manufacturing (AM) without any further post processing of the channel.

In the first test constant losses are induced in each segment to simulate an even power loss distribution and to compare the aluminum DUT to the steel DUT.

In a second test the influence of distributed power losses is investigated, with the DUT made from aluminum 7075.

Verification of the Measurements

After each measurement, the plausibility checks are done first. For this the previously mentioned check of the resulting pressure drop is performed. For a flow rate of 5 l/min, a drop of 30 Pa is expected. The measured pressure drop for the steel DUT at 5 l/min is 30 Pa, which matches the previous calculations.

For verifying the power flow, the measurements are veryfied using Equation (8). Here the measurement results in an average temperature difference of 1.3 K, with a coolant flow rate of 5 l/min and set power losses of 700 W, instead of the expected 2 K from the calculation. Applying Eqation (8) this is equivalent to 450 W power losses. Whereas for losses of 1400 W a ΔT of 2.6 K is measured being equivalent to 900 W.
This effect stems from layering of the coolant, as depicted in Figure 6 in a qualitative way. At the bottom, the coolant is hotter (red) than in the area of measurement where the coolant is cooler (green). For a correct verification, the mixing temperature across the whole channel is needed. This effect will be further looked into and ways for proper measurement going to be evaluated.

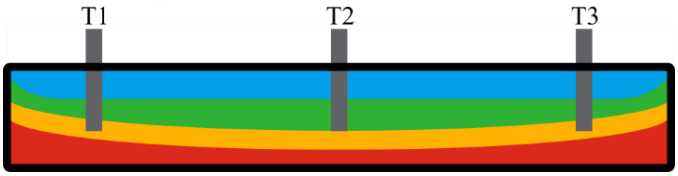

Figure 6 Qualitative temperature cross section of the channel with layering

Influence of Material on Absolute Temperature Levels

The mechanical and thermal properties for both materials can be found in the Appendix - Table 3.

The DUTs are mounted on the heating plate and a linear loss profile is induced, with each heating cartridge set to 100 W summing up to $P_{losses} = 7 \text{ x } 100 \text{ W} = 700 \text{ W}$, representing the S1-operating point of the reference motor. The measurements are performed at 5 l/min in a thermal stationary state where the temperatures are at an equilibrium.

In Figure 7, the temperature for the aluminum DUT is shown in blue. As can be seen for the dotted line, representing 7 x 100 W, the temperature difference ΔT from inlet to outlet is 10 K. With the losses set to 7 x 200 W, the ΔT rises up to 18 K.
When performing the same measurements for the stainless steel

DUT, a ΔT of 18 K can be observed for 7x100 W and for 7x200 W the difference is even 25 K.

When comparing the highest temperatures of the steel DUT to the aluminum DUT, a difference of 9.5 K in the 7x100 W scenario and 17 K in the 7x200 W scenario can be observed.

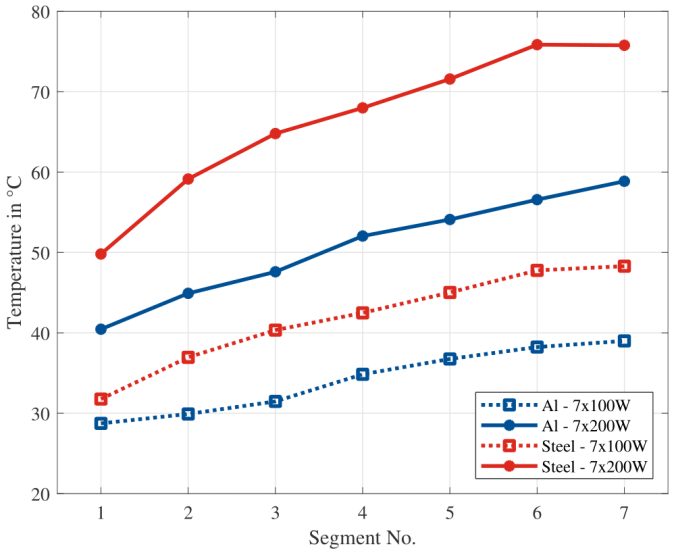

Figure 7 Temperature profile using different materials at 5 l/min.

Influence of Distributed Losses

In the following test, the diffent temperature distribution is investigated, using the aluminum 7075 DUT. For this the heating cartridges at the beginning and at the end (cartridge 1 and 7, Figure 5) are set to a different power level than the ones in the middle. As basis for this, a loss distribution of up to 20 % end winding losses, as stated in [7], is assumed. Resulting in a heating power of 150 W for the first and last cartridge. For the measurement to be comparable to the linear distribution a total loss of 700 W is aspired. This results in 80 W for the other five cartridges resulting with a total power loss of 1x150 W + 5x80 W + 1x150 W = 700 W. The result of the measurement can be seen in Figure 8, where the blue dotted profile is showing the temperatures in the segments for a linear power loss profile and the red line for the distributed power loss profile.

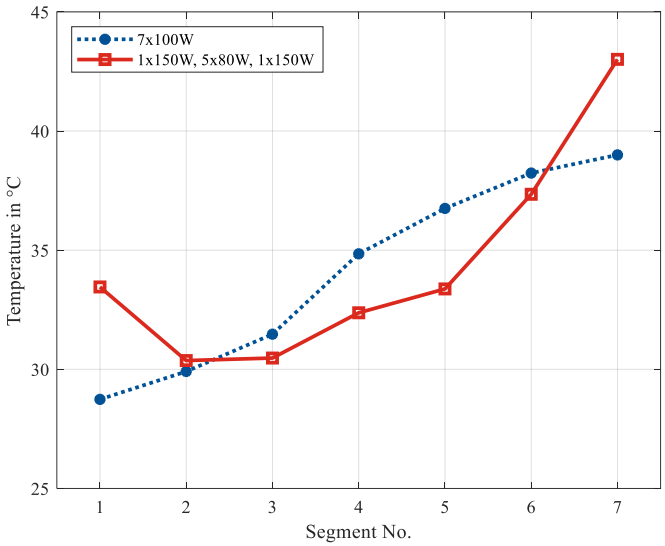

Figure 8 Temperature profile in aluminum DUT- linear vs. distributed losses at 5 l/min.

As can be seen in Figure 8, the mayor changes in the temperature distribution is in the first and last segment. Compared to the linear distribution, the temperature at the inlet is increased by 4 K and at the outlet by 5 K. The maximum temperature difference ΔT, which is now present between segments 2 and 7 and not 1 to 7, is increased from 10 K to 13 K.

Discussion

When looking at the previously presented results, a few conclusions can be made and further research topics can be distinguished.

When comparing DUTs made from different materials, the steel version is less effective with an unmodified geometry. The reason for thi is mainly due to the higher thermal capacity and lower thermal conductivity of the steel. Further engineering design changes can be potentially implemented to use the higher tensile and ductile strength of steel in comparison to aluminum to drastically reduce wall thickness. With much thinner walls the lower thermal conductivity for steel can be compensated. There is also the possibility to design a smaller electric motor than with the use of aluminum. This will lead to a higher volumetric power density. Another benefit of a steel cooling jacket is as that the active stator material is iron based and thus the thermal expansion of both components are more aligned.

As can be seen from both experiments, there is a significant temperature gradient present as well as hotspots. Reducing the hotspots can help in various ways:

- Power derating of the electric machines due to high temperatures at hotspots can be delayed, resulting in a better thermal utilization of the whole electric motor.
- There is the possibility to use cheaper insulating materials or magnets, when i.e. a reduction of 13 K at hotspots is possible, as shown in the previous chapter
- Reduction of the overall build volume and increase of volumetric power density.
- Higher continuous power output, if the volume is held constant.

Conclusions

In this paper, the necessity of cooling for high power density drives is presented, as well as various state of the art cooling systems in electric motors and power electronics.

The measurements show, that a noteworthy temperature gradient is present along cooling channels when the cooling system is based on a global and thus constant channel geometry. This is even more amplified by distributed power losses presented in this paper.

Based on this, it is shown that there a need for systematic evaluation of zonal optimized cooling structures to improve thermal machine design.

The next steps to increase the reliability of the statements are:

- Measurement of thermal properties of materials with finite bars.
- Implementation of a pinhole for a defined pressure drop before and after the cooling channel to homogenize the flow and mix the coolant for proper averaged coolant temperature.
- Optimization of measurement procedures to increase accuracy, especially for fluid temperature.
- Investigation of pressure drop regarding surface roughness (Ra).
- Reduction of temperature profile using adaptive positioning of cooling structures.

References

[1] Heckmann, M., "Vergleichende Untersuchungen an hydraulischen undelektrischen Achsantrieben für mobile Arbeitsmaschinenunter Berücksichtigung betriebstypischer Einsatzbedingungen," Dissertation, Universitätsbibliothek der Technischen Universität München, München, 2015.

[2] Geimer, M., "Mobile Working Machines," Society of Automotive Engineers. Electronic publications, SAE International, Warrendale, Pa., ISBN 9780768099546, 2020.

[3] Dimier, T., Cossale, M., and Wellerdieck, T., "Comparison of Stator Winding Technologies for High-Speed Motors in Electric Propulsion Systems," *Proceedings 2020 International Conference on Electrical Machines (ICEM): Online, 23-26 August, 2020*, 2020 International Conference on Electrical Machines (ICEM), Gothenburg, Sweden, 8/23/2020 - 8/26/2020, IEEE, Piscataway, NJ, ISBN 978-1-7281-9945-0:2406–2412, 2020.

[4] Sun, Y., Zhang, S., Yuan, W., Tang, Y. et al., "Applicability study of the potting material based thermal management strategy for permanent magnet synchronous motors," *Applied Thermal Engineering* 149:1370–1378, 2019, doi:10.1016/j.applthermaleng.2018.12.141.

[5] Svetlana Zhitkova, Björn Riemer, David Franck, Kay Hameyer et al., "Hochdrehzahlmotoren für mobile Arbeitsmaschinen," in: Geimer, M., Synek, P.-M., and Institut für Fahrzeugsystemtechnik (eds.), *Hybridantriebe für mobile Arbeitsmaschinen: 4. Fachtagung [des VDMA und des Karlsruher Instituts für Technologie], 20. Februar 2013, Karlsruhe*, Karlsruher Schriftenreihe Fahrzeugsystemtechnik, KIT Scientific Publishing, Karlsruhe, ISBN 978-3-86644-970-1:113–123, 2013.

[6] Epskamp, T., "Steigerung der Leistungsdichte von Traktionsantrieben und Aufbau einer hochdrehenden Asynchronmaschine," 2020, doi:10.5445/IR/1000117913.

[7] Acquaviva, A., Wallmark, O., Grunditz, E.A., Lundmark, S.T. et al., "Computationally Efficient Modeling of Electrical Machines With Cooling Jacket," *IEEE Trans. Transp. Electrific.* 5(3):618–629, 2019, doi:10.1109/TTE.2019.2936122.

[8] Huber, A., Nguyen-Xuan, T., Brossardt, N., Eckstein, F. et al., "Thermische Simulation eines hochdetaillierten Wickelkopfmodells einer elektrischen Antriebsmaschine," ANSYS Conference & 32. CADFEM Users' Meeting 2014, Nürnberg, June 4, 2014.

[9] Gronwald, P.-O. and Kern, T.A., "Traction Motor Cooling Systems: A Literature Review and Comparative Study," *IEEE Transactions on Transportation Electrification* 7(4):2892–2913, 2021, doi:10.1109/TTE.2021.3075844.

[10] Yang, X., Fatemi, A., Nehl, T., Hao, L. et al., "Comparative Study of Three Stator Cooling Jackets for Electric Machine of Mild Hybrid Vehicle," *2019 IEEE International Electric Machines & Drives Conference (IEMDC)*, 2019 IEEE International Electric Machines & Drives Conference (IEMDC):1202–1209, 2019.

[11] Wrobel, R., "A technology overview of thermal management of integrated motor drives – Electrical Machines," *Thermal Science and Engineering Progress* 29:101222, 2022, doi:10.1016/j.tsep.2022.101222.

[12] Huber, A., Pfitzner, M., Nguyen-Xuan, T., and Eckstein, F., "Effiziente Strömungsführung im Wassermantel elektrischer Antriebsmaschinen," *ATZelektronik* 8(6):478–485, 2013, doi:10.1365/s35658-013-0370-8.

[13] Karras, N., "Optimierung der Wärmeabfuhr eines Fahrzeug-Elektromotors und Auswirkungen auf den Gesamtkühlkreislauf," Dissertation, Universität Stuttgart, Stuttgart, 2017.

[14] Feikus, F.J., Bernsteiner, P., Gutiérrez, R.F., and Łuszczak, M., "Weiterentwicklungen bei Gehäusen von Elektromotoren," *MTZ Motortech Z* 81(3):42–47, 2020, doi:10.1007/s35146-019-0180-5.

[15] Hanno Jelden,Peter Lück, Georg Kruse, Jonas Tousen, "Der elektrische Antriebsbaukasten von Volkswagen," *MTZ - Motortechnische Zeitschrift* 2014(2):14–20, 2014.

[16] Drescher, U., "Innengekühlte Hohldrähte verdoppeln die Leistungsdichte von E-Motoren," *konstruktionspraxis*, 2020.

[17] Schiefer, M. and Doppelbauer, M., "Indirect slot cooling for high-power-density machines with concentrated winding," *2015 IEEE International Electric Machines & Drives Conference (IEMDC)*, 2015 IEEE International Electric Machines & Drives Conference (IEMDC), Coeur d'Alene, ID, 10.05.2015 - 13.05.2015, IEEE, ISBN 978-1-4799-7941-7:1820–1825, 2015.

[18] Wrobel, R. and McGlen, R.J., "Opportunities and Challenges of Employing Heat-Pipes in Thermal Management of Electrical Machines," *Proceedings 2020 International Conference on Electrical Machines (ICEM): Online, 23-26 August, 2020*, 2020 International Conference on Electrical Machines (ICEM), Gothenburg, Sweden, 8/23/2020 - 8/26/2020, IEEE, Piscataway, NJ, ISBN 978-1-7281-9945-0:961–967, 2020.

[19] Chen, J., Müller-Steinhagen, H., and Duffy, G.G., "Heat transfer enhancement in dimpled tubes," *Applied Thermal Engineering* 21(5):535–547, 2001, doi:10.1016/S1359-4311(00)00067-3.

[20] Bae, J.C., Cho, H.R., Yadav, S., and Kim, S.C., "Cooling Effect of Water Channel with Vortex Generators on In-Wheel Driving

Motors in Electric Vehicles," *Energies* 15(3):722, 2022, doi:10.3390/en15030722.
[21] Al-Neama, A.F.M., "Serpentine Minichannel Liquid-Cooled Heat Sinks for Electronics Cooling Applications," Dissertation, The University of Leeds, Leeds, 2018.
[22] "DIN EN IEC 60751:2019-09, Industrielle Platin-Widerstandsthermometer und Platin-Temperatursensoren (IEC_65B/1144/CD:2018); Text Deutsch und Englisch," Beuth Verlag GmbH.
[23] Verein Deutscher Ingenieure, "VDI heat atlas," Springer reference, 2nd ed., Springer, Berlin, Heidelberg, ISBN 978-3-540-77876-9, 2010.

Acknowledgements

"This Project is supported by the Federal Ministry for Economic Affairs and Climate Action (BMWK) on the basis of a decision by the German Bundestag."

Contact Information

Christoph Ellenrieder, M.Sc. – christoph.ellenrieder@rwu.de
Ravensburg-Weingarten University
88250 Weingarten
Germany

Definitions/Abbreviations

DUT	device under test
Ra	Arithmetic average roughness of surface texture
CFD	Computational fluid dynamics
NACA	National Advisory Committee for Aeronautics
EDM	Electric discharge machining
AM	Additive manufacturing

Appendix

Table 3 Material Parameters of Used Metals

Material	Density $\frac{kg}{m^3}$	Specific Heat Capacity $\frac{J}{kg \cdot K}$	Thermal Conductivity $\frac{W}{m \cdot K}$	Coefficient of thermal expansion $\frac{1}{K \cdot 10^6}$
EOS Stainless Steel NX [1] Cr11Ni8	7690	460 (estimated)	21 (estimated)	11.6
Aluminium 7075 [2]	2800	862	130 - 160	23.4

ISSN 0148-7191
https://saemobilus.sae.org/content/2022-24-0007

[1] https://www.eos.info/03_system-related-assets/material-related-contents/metal-materials-and-examples/metal-material-datasheet/stainlesssteel/material_datasheet_eos_stainlesssteel_cx_premium_en_web.pdf

[2] https://datenblaetter.thyssenkrupp.ch/en_aw_7075_0717.pdf